

techniques available at kilohertz repetition rates offer the potential for attosecond-resolution atomic spectroscopy and nonlinear optics in the x-ray regime.

REFERENCES AND NOTES

- J. C. Solem and G. C. Baldwin, *Science* **218**, 229 (1982); M. Howells *et al.*, *ibid.* **238**, 514 (1987); J. E. Trebes *et al.*, *ibid.*, p. 517.
- D. Attwood, K. Halbach, K.-J. Kim, *ibid.* **228**, 1265 (1985).
- B. J. Macgowan *et al.*, *Phys. Rev. Lett.* **65**, 420 (1990).
- Flash x-ray sources such as those demonstrated in (3) would be ideal for the avoidance of image blurring due to, for example, object motion during exposure [R. A. London *et al.*, *Appl. Opt.* **28**, 3397 (1989)]; however, the spatial coherence of the sources demonstrated in the water window so far are far from being sufficient for single-shot biological holography.
- A. McPherson *et al.*, *J. Opt. Soc. Am. B* **4**, 595 (1987); X. F. Li *et al.*, *Phys. Rev. A* **39**, 5751 (1989).
- A. L'Huillier and Ph. Balcou, *Phys. Rev. Lett.* **70**, 774 (1993); J. J. Macklin *et al.*, *ibid.*, p. 766.
- J. L. Krause *et al.*, *ibid.* **68**, 3535 (1992).
- P. B. Corkum, *ibid.* **71**, 1995 (1993).
- M. Lewenstein *et al.*, *Phys. Rev. A* **49**, 2117 (1994).
- K. C. Kulander *et al.*, in *Proceedings of the Workshop on Super-Intense Laser Atom Physics (SILAP) III*, P. Piraux, Ed. (Plenum, New York, 1993).
- K. Miyazaki and H. Takada, *Phys. Rev. A* **52**, 3007 (1995).
- I. P. Christov *et al.*, *Phys. Rev. Lett.* **77**, 1743 (1996); K. J. Schafer and K. C. Kulander, *ibid.* **78**, 638 (1997).
- J. Zhou *et al.*, *ibid.* **76**, 752 (1996).
- Z. Chang *et al.*, in *Applications of High Field and Short Wavelength Sources VII* (OSA Tech. Digest Ser., vol. 7, Optical Society of America, Washington, DC, 1997), p. 187.
- R. Haight and P. F. Seidler, *Appl. Phys. Lett.* **65**, 517 (1994).
- S. Sartania *et al.*, *Opt. Lett.* **22**, 1562 (1997).
- M. Nisoli *et al.*, *ibid.*, p. 522.
- Given the finite tube wall thickness of 0.05 mm, the actual target thickness is estimated as 100 to 200 μm . The coherence length related to the phase error introduced by the tight focusing of the fundamental (1) is on the order of 10 μm for wavelengths shorter than 10 nm. The target thickness has been minimized in an attempt to keep the interaction length as close as possible to this "geometric" coherence length. It is this geometric coherence length limitation that dictates the necessity of the high pressures applied.
- Note that this peak irradiance is reached only on the propagation axis in an infinitesimally small fraction of the cross section of the Gaussian beam. The majority of the helium atoms in the interaction volume are exposed to somewhat lower irradiances.
- The pressure in the interaction region has been estimated as follows. The gas flow from the target region into the chamber is calculated from the known pumping speed and the measured background pressure in the target chamber. Gas flow and background pressure then determine uniquely the pressure in the target.
- I. P. Christov *et al.*, *Phys. Rev. Lett.* **78**, 1251 (1997).
- C. Kan *et al.*, *ibid.* **79**, 2971 (1997).
- We used a detector quantum efficiency of 2%, an electron multiplication gain of 5×10^6 , and a grating diffraction efficiency of 10% (data provided by the manufacturers) for this estimation.
- M. Schnürer *et al.*, unpublished results.
- M. V. Ammosov *et al.*, *Zh. Eksp. Teor. Fiz.* **91**, 2008 (1986) [*Sov. Phys. JETP* **64**, 1191 (1986)].
- Siegman *et al.*, *IEEE J. Quantum Electron.* **27**, 1098 (1991).
- Measurement of the x-ray beam profile at different positions or direct interferometric measurement of its spatial coherence will obviate the need for this assumption.
- C. Kan and N. H. Burnett, unpublished results.
- The electric field of a light pulse can be described in terms of a carrier of frequency ω_0 and a time-varying envelope of amplitude $A(t)$: $E(t) = A(t) \exp[-i(\omega_0 t + \psi)]$. This decomposition can be used to pulse durations down to the carrier oscillation cycle [T. Brabec and F. Krausz, *Phys. Rev. Lett.* **78**, 3282 (1997)]. The parameter ψ is the relative carrier phase. It determines the position of the carrier with respect to the envelope.
- L. Xu *et al.*, *Opt. Lett.* **21**, 2008 (1996).
- We are indebted to A. J. Schmidt for his encouragement and T. Brabec for useful discussions. K. Ferencz (Research Institute for Solid State Physics, Budapest, Hungary) is gratefully acknowledged for manufacturing the silver foils. This research was supported by the Austrian Science Foundation under grants P-11109 and Y44-PHY.

21 May 1997; accepted 9 September 1997

Superfluid Droplets on a Solid Surface

D. Ross, J. E. Rutledge, P. Taborek*

Photographs are presented of isolated superfluid helium-4 droplets prepared on a cesium surface, the only material known that is not wetted by superfluid helium. Although thermodynamic measurements show that the cesium surface is highly uniform, the contact angle of the droplets is extremely hysteretic and depends on whether the contact line is advancing or receding. Superfluid helium-4 droplets on an inclined surface do not flow downhill but rather are strongly pinned to the surface.

Superfluid He has unusual thermal and mechanical properties (1) and is well known for its ability to spread over surfaces and to flow without dissipation through even microscopic holes. Virtually all of the walls and surfaces used in earlier dissipationless flow experiments were observed to be wetted by superfluid He. This effect means that droplets on these substrates are unstable and immediately spread to form a smooth continuous film over the entire surface so that vapor and substrate are never in contact. Recent work (2) has shown that alkali metals are a special class of materials not completely wetted by superfluid He. In particular, Cs substrates can be used to prepare superfluid samples with a distinctly different topology consisting of a droplet with an edge where substrate, superfluid, and vapor meet at a three-phase contact line (3). We present here direct observations of isolated droplets of superfluid on a substrate (4). Both the static and the dynamic behaviors of the droplets were unusual. We found that the contact angle was an extremely hysteretic function of the volume of the drop. Perhaps most remarkable, superfluid droplets would not move across the surface until considerable force was applied to them. This result is surprising because solid surfaces are well known not to exert transverse forces on bulk superfluid or superfluid films without edges.

Our apparatus consisted of a substrate that can be rotated about a horizontal axis mounted in an optical cryostat with win-

dows that provide an edge-on view of the substrate as well as a view from above at an angle of 60° from the normal. The substrate is a quartz microbalance with gold electrodes similar to those used in our earlier thermodynamic studies (5, 6). Fifty atomic layers of Cs were vapor-deposited onto the quartz and gold surfaces of the microbalance at a rate of 0.01 layer per second. During the evaporation, the temperature of the substrate and the walls of the container were maintained below 6 K to maintain ultrahigh vacuum conditions. We used the microbalance to monitor the deposition and to perform thermodynamic characterizations of the surface; the wetting temperature was measured to be $T_w = 2.04$ K. A capillary tube (0.04 cm, outside diameter) attached to a source of room-temperature gas through a mass-flow controller provided a means of putting drops of superfluid on the surface. We maintained the system at liquid-vapor coexistence by filling the bottom of the container with bulk liquid ^4He . The drops were observed with a long-focal-distance microscope that provided a magnification of $\sim \times 30$.

Figures 1 and 2 show a sequence of photos of superfluid drops on a Cs substrate at $T = 1.16$ K. Pictures taken with the microscope looking down on the substrate at an angle of 30° above the horizontal are shown in Fig. 1. The dark bar at the top of the pictures is the capillary tube, and the lower bar is its shadow. The tube was left in contact with the superfluid drop so that fluid could be added and withdrawn. This geometry is conventional for contact-angle measurements and typically yields the advancing and receding

Department of Physics and Astronomy, University of California, Irvine, CA 92697, USA.

*To whom correspondence should be addressed.

contact angle (7). The drops appear oval because of the viewing angle. The edge of the planar gold electrode can be seen in the extreme and upper left; the Cs film is too thin to provide appreciable optical contrast. Figure 2 shows edge-on views of the same droplets as shown in Fig. 1 illuminated from the back. The optical axis is a fraction of a degree above the horizontal, so that both the free surface of the drop and its reflection in the substrate are visible. The capillary tube can be seen protruding from the top of the drop. The focus was adjusted so that a diameter of the drop lies in the focal plane.

One can locate the plane of the substrate by drawing a line between the two points where the profile of the drop meets its mirror image. The contact angle is the angle between the tangent to the drop profile and the substrate at the point of contact. Despite the superfluidity of the drops, the value of the contact angle that we observed depended critically on the way the drop was prepared. When the volume of the drop was increasing, the contact angle

was about 32° (8) and independent of the volume of the drop; Fig. 2, A and B, show snapshots of the same drop as fluid was added (the corresponding top view of the growing drop is shown in Fig. 1, A and B). When fluid was withdrawn, the contact line remained stationary, and the receding contact angle approached zero (Figs. 1C and 2C). The bulk fluid could be completely removed, but apparently a thin film remained in the region bounded by the original contact line, because, when fluid was added, the drop immediately resumed its previous diameter and only slowly increased its volume and contact angle. The only way to prepare a smaller drop (such as Fig. 1A) in the same area was to remove the microscopic film by briefly heating the substrate with a flash of light.

Contact-angle hysteresis is a common phenomenon in wetting measurements of conventional liquids and substrates that is typically attributed to substrate heterogeneity or kinetic effects associated with the viscosity of the liquid, or both (7, 9, 10). Because our experiment used superfluid and the time scale of the observations was several minutes, kinetics cannot be invoked to explain the hysteresis we observed. Similarly, it is difficult to find a plausible source of surface heterogeneity, because the substrate exhibits the same sharp thermodynamic signatures of the

wetting transition that we have explored in previous work (5, 6). In order to explain a receding contact angle of zero, standard models based on consideration of metastable states on a heterogeneous substrate would require that more than half of the surface be covered with patches where the local contact angle is zero, that is, where the liquid wets (7, 10). This possibility is ruled out by microbalance measurements that show that the average equilibrium coverage at liquid-vapor coexistence on our substrate at temperatures far below the wetting temperature is less than two monolayers, which implies that the fraction of the surface that was wetted is less than 4%. The possibility of point-like pinning centers also seems unlikely because the contact line (Fig. 1) appears perfectly smooth on length scales of a few micrometers.

Although the conventional explanations of contact-angle hysteresis due to surface heterogeneity do not apply to our experiment, there must nevertheless be some mechanism that provides metastable states that can trap the droplet in configurations with a continuous range of contact angles. The fact that the contact line did not move even when the apparent contact angle was reduced to zero as a result of the deflation of the drop allows us to place a lower limit on the pinning force per unit length that these metastable states can sustain. We assume, as is customary, that the advancing contact angle is equal to the thermodynamic equilibrium contact angle θ (8), which satisfies Young's equation

$$\sigma_{lv}\cos\theta = \sigma_{sv} - \sigma_{sl}$$

where the σ_{ij} are surface tensions, and the l , s , and v subscripts denote liquid, substrate,

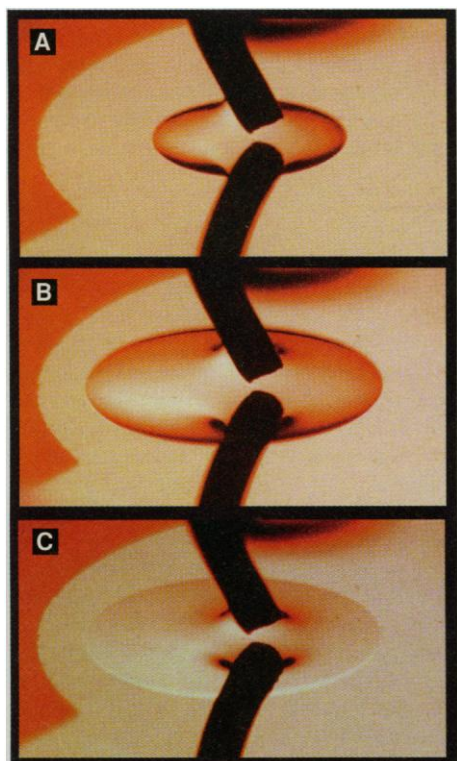


Fig. 1. (A through C). Microscope images of superfluid drops on a horizontal Cs substrate taken at an angle of 30° above the horizontal. The two dark bars in each of these pictures are the capillary tube used to add and remove superfluid (top) and its shadow, respectively. The capillary is in wetting contact with the drop. From (A) to (B), fluid was added; from (B) to (C), fluid was withdrawn. The edges of the drop were always smooth, and the footprint of the drop did not change size when fluid was withdrawn.

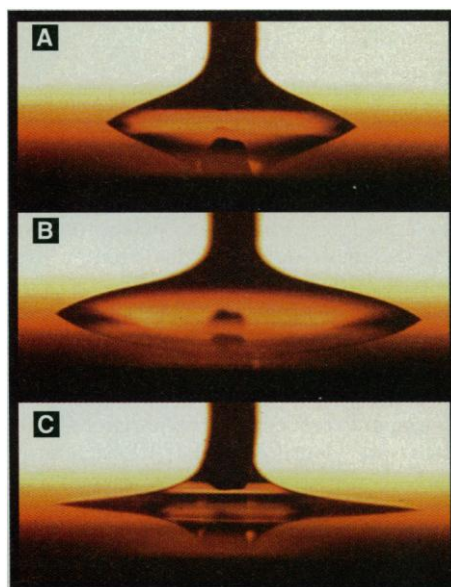


Fig. 2. (A through C) Microscope images showing an edge-on view of superfluid drops on a horizontal Cs substrate. The dark bar in the upper half of the image is the capillary tube. The pictures show the outline of the drop as well as its mirror image in the reflective substrate. As the volume of the drop increased from (A) to (B), the contact angle remained constant. When fluid was withdrawn as in (C), the contact angle decreased but the diameter remained constant.



Fig. 3. Microscope image of a superfluid drop on a Cs substrate inclined at 10° to the horizontal. A drop hanging off of the capillary is also seen in the upper right. The drop on the inclined substrate is stationary. The downhill edge of the drop has the same contact angle as shown in Fig. 2B, whereas the uphill edge has a vanishing contact angle.

and vapor, respectively. In this case, the force per unit length on the contact line due to surface tension when the contact angle was reduced to zero was $\sigma_w(1 - \cos\theta) \approx 46$ mdyne/cm. The maximum pinning force must be at least as large.

Another manifestation of forces on the contact line can be seen when a superfluid drop was placed on an inclined surface. Figure 3 shows an edge-on view of a drop on a Cs surface inclined at $\sim 10^\circ$ to the horizontal; a pendant drop of fluid formed by forcing He down the capillary faster than the superfluid film on the outer surface could drain it can also be seen in the upper right corner. The most remarkable feature of the drop on the substrate is that it is stationary. Even vigorous shaking of the apparatus, which caused easily discernible waves in the drop, did not cause it to flow down the incline. The downhill edge of the drop had the same contact angle as the advancing edge of a growing drop, whereas the uphill edge had a vanishing contact angle. As more fluid was added to the drop, it eventually rolled down the incline, often with a jerky stick-slip motion. Subsequent drops immediately spread out across the path of the previous drop and rapidly flowed downhill. It seems as if the first drop, which moved across a dry substrate, left a trailing film that "lubricates" the motion of subsequent drops. This film, which persisted for hours, may be related to the metastable thick films we have observed in earlier experiments (6). The trailing film had submicroscopic thickness and was invisible in an edge-on view. It could be detected ellipsometrically and was superfluid because the local heating of a spot with a laser beam produced a thermomechanically driven bump in the film profile.

Superfluid droplets on Cs substrates have spreading and flow properties that are not simple consequences of bulk superfluid behavior. Liquid He has exceptional chemical purity, and the heterogeneity of our Cs surface is constrained by thermodynamic adsorption measurements. For these reasons, He on Cs would naïvely be expected to display nearly ideal reversible spreading behavior, because even the complications due to viscosity are negligible. In contrast, superfluid contact angles are found to be even more hysteretic than typical classical fluid drops on macroscopically heterogeneous surfaces. The hysteresis is so extreme that the superfluid contact line appears to move in only one direction, that is, so as to increase the wetted area.

It is difficult to reconcile these observations with standard models of contact-angle hysteresis. Regarded as a superfluid, droplets

are remarkable because they can resist flow against a substantial chemical potential gradient. Both of these effects are presumably due to metastable configurations of the superfluid contact line, which have been inaccessible to experimental observation until very recently. In order to attribute the metastability to extrinsic defects, a mechanism that would allow small defect concentrations to cause extremely large hysteresis would need to be identified.

REFERENCES AND NOTES

1. J. Wilks and D. S. Betts, *An Introduction to Liquid Helium* (Clarendon Press, Oxford, ed. 2, 1987).
2. E. Cheng, M. W. Cole, J. Dupont-Roc, W. F. Saam, J. Treiner, *Rev. Mod. Phys.* **65**, 557 (1993), and references therein.

3. F. Brochard-Wyart, *J. Phys. (Paris) II* **3**, 21 (1993).
4. D. Reinelt, H. Gau, S. Herminghaus, P. Leiderer [*Czech. J. Phys.* **46**, 431 (1996)] presented surface plasmon micrographs of the region of a Cs substrate covered with superfluid. These images, however, did not contain information about the contact angle.
5. J. E. Rutledge and P. Taborek, *Phys. Rev. Lett.* **69**, 937 (1992).
6. P. Taborek and J. E. Rutledge, *ibid.* **71**, 263 (1993).
7. R. E. Johnson and R. H. Dettre, in *Wettability*, J. C. Berg, Ed. (Dekker, New York, 1993), pp. 1–73.
8. The contact angle has been measured by J. Klier, P. Stefanyi, and A. F. G. Wyatt [*Phys. Rev. Lett.* **75**, 3709 (1995)]. They obtained a slightly larger value at $T = 1.16$ K.
9. D. Li and A. W. Neumann, *Colloid Polym. Sci.* **270**, 498 (1992).
10. L. W. Schwartz and S. Garoff, *Langmuir* **1**, 219 (1985).
11. This work was supported by NSF grant DMR 9623976.

7 July 1997; accepted 15 September 1997

Developmental Patterns and the Identification of Homologies in the Avian Hand

Ann C. Burke and Alan Feduccia*

Homologies of digits in the avian hand have been debated for 150 years. Cladistic analysis nests birds with theropod dinosaurs. Theropod hands retain only digits I-II-III, so digits of the modern bird hand are often identified as I-II-III. Study of the developing manus and pes in amniote embryos, including a variety of avian species, shows stereotyped patterns of cartilage condensations. A primary axis of cartilage condensation is visible in all species that runs through the humerus into digit IV. Comparison to serially homologous elements of the hindlimb indicates that the retained digits of the avian hand are II-III-IV.

A long-standing disagreement persists in the identification of the three remaining digits in the adult avian manus. Many developmental biologists use conservation of embryonic patterning to establish homology (1, 2), while many paleontologists use the methodology of phylogenetic systematics to define homology a posteriori from cladistic analysis of multiple synapomorphies (3, 4). Cladistic analyses nest birds within the theropod dinosaurs (5). One key synapomorphy uniting theropods is a manus reduced to three digits. These digits are identified as I-II-III because of early theropods such as *Herrerasaurus* (Fig. 1) that show dramatic reduction of digits IV and V (6). A theropod origin of birds implies that the digits of the avian manus must also be I-II-III (7, 8). However, neontologists have identified the digits in the avian hand as II-III-IV in consideration of developmental anatomy. Despite several excellent descriptive studies (2, 9)

and thorough reviews of the arguments (1, 8, 10, 11), no consensus on digit homology has emerged. We address the issue of avian digits, using a developmental pattern that is conserved in all amniotes examined. We examined forelimb development in turtle, alligator, and several avian embryos (12). We also compare development of the serially homologous fore- and hindlimbs in birds.

The identity of digits in modern birds as I-II-III gained acceptance because the phalangeal formula of *Archaeopteryx*, an undisputed early avian (13), coincides with digits I-II-III of the generalized archosaur hand [2-3-4-5-3 (14)]. Phalangeal formulae are widely variant among many taxa, however, and individual specimens of *Archaeopteryx* have varying phalangeal formulae in the pes (15). Furthermore, this character is developmentally plastic. For example, bone morphogenetic protein 4 (BMP4) mediates apoptosis and recent studies have shown that experimental blockage of BMP4 signaling in the avian limb bud can result in hands that are missing only the most distal phalanxes (16). Regardless, the transition to modern

Department of Biology, Coker Hall, Campus Box 3280, University of North Carolina, Chapel Hill, NC 27599–3280, USA.

*To whom correspondence should be addressed.